Mechanistic Insights on Spontaneous Moisture-Driven Healing of Urea-Based Polyurethanes

Bertrand Willocq,[†] Farid Khelifa,[†] Jeremy Odent,[†] Vincent Lemaur,[‡] Ying Yang,[§] Philippe Leclère,[‡] Jérôme Cornil,[‡] Philippe Dubois,[†] Marek W. Urban,[§] and Jean-Marie Raquez*,[†]

[†]Laboratory of Polymeric and Composite Materials (LPCM), Center of Innovation and Research in Materials and Polymers (CIRMAP) and [‡]Laboratory for Chemistry of Novel Materials, Center for Research in Molecular Electronics and Photonics, University of Mons, Place du Parc 23, B-7000 Mons, Belgium

[§]Department of Materials Science and Engineering and Center for Optical Materials Science and Engineering Technologies (COMSET), Clemson University, P-4-19, Anderson, South Carolina 29634, United States

Ⓢ *Supporting Information*

ABSTRACT: Self-healing polymeric materials that can spontaneously repair in a perpetual manner are highly appealing to address safety and restoration issues in different key applications. Usually built from reversible moieties that require to be activated using, for example, temperature, light, or pH changes, most of these self-healing materials rely on energy-demanding processes and/or external interventions to promote self-healing. In this work, we propose to exploit rapid dynamic exchanges between urea-based moieties and moisture as an alternative to promote local and spontaneous healing responses to damage using atmospheric moisture as an external stimulus. Non-hygroscopic urea-based polyurethanes with repetitive moisture-induced healing abilities at different degrees of humidity were thus designed through coupling reactions with non-hygroscopic polypropylene glycol and urea moieties. As supported by density functional theory (DFT) calculations coupled to local FTIR experimental studies, we furthermore established that the healing mechanism is ultimately related to the formation of water−urea clusters. Obviously, this work represents a platform for designing more advanced spontaneous self-healing materials beyond the present study, which hold promise for use in a wide range of technological applications.

KEYWORDS: Self-healing, Spontaneous, Moisture, Urea, Polyurethanes
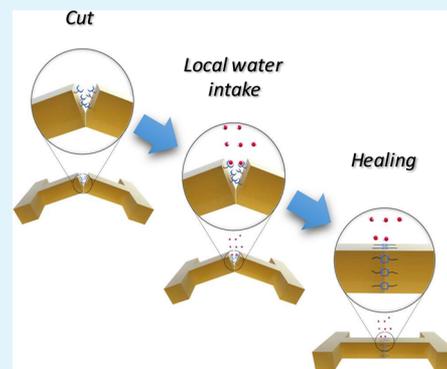
■ INTRODUCTION

The 21st century has witnessed the emergence of advanced polymeric materials in response to societal, environmental, and technological challenges. Yet, the long-lasting performances of advanced materials represent a major issue as they are subjected to severe load-bearing and aggressive external conditions during their lifetime. Self-healing polymeric materials that can spontaneously repair in a perpetual manner are therefore highly appealing to address these safety and restoration issues.

Biomimicry has surely represented the major inspiration pool for numerous researchers to design advanced materials with autonomous self-healing properties, yet this approach is not trivial.[1] That is, autonomous self-repairing in polymers implies both adequate combination of physical/chemical concerted events and the use of specific stimulus-responsive moieties.[2,3] Major breakthroughs have been achieved on the implementation of reversible chemistry into polymeric materials such as Diels−Alder reactions and UV-light cycloadditions, though most of them rely on energy-demanding processes and/or external interventions to promote self-healing. An attractive alternative is to design polymeric materials that can spontaneously and repeatedly self-repair under ambient conditions,

particularly using atmospheric humidity and/or CO_2. This concept has been scarcely explored, except the very few examples of water-induced self-repairing of polymers after purposely wetting and drying the scratched surface. As such, Koschek et al. reported moisture-induced healing of highly cross-linked poly(urea-urethane) films containing 1-(2-amino-ethyl) imidazolidone, however the healing efficiency was only determined based on coating scratch recovery.[4,5] Inspired by the chemistry of adhesive proteins in mussels, hydrogels that are able to heal in water were also demonstrated.[6−11] Liu et al. reported silicone-based materials with water-enhanced healing built from multiphase-assembled siloxane oligomers through multivalent hydrogen bonding.[12] The low water permeability of the as-designed materials allows environmental water molecules to travel through the siloxane network to help dissociation of the multivalent hydrogen bonds to achieve rapid healing with high efficiency. In another work, Cash et al. reported materials exhibiting healing capabilities under wet conditions based on the
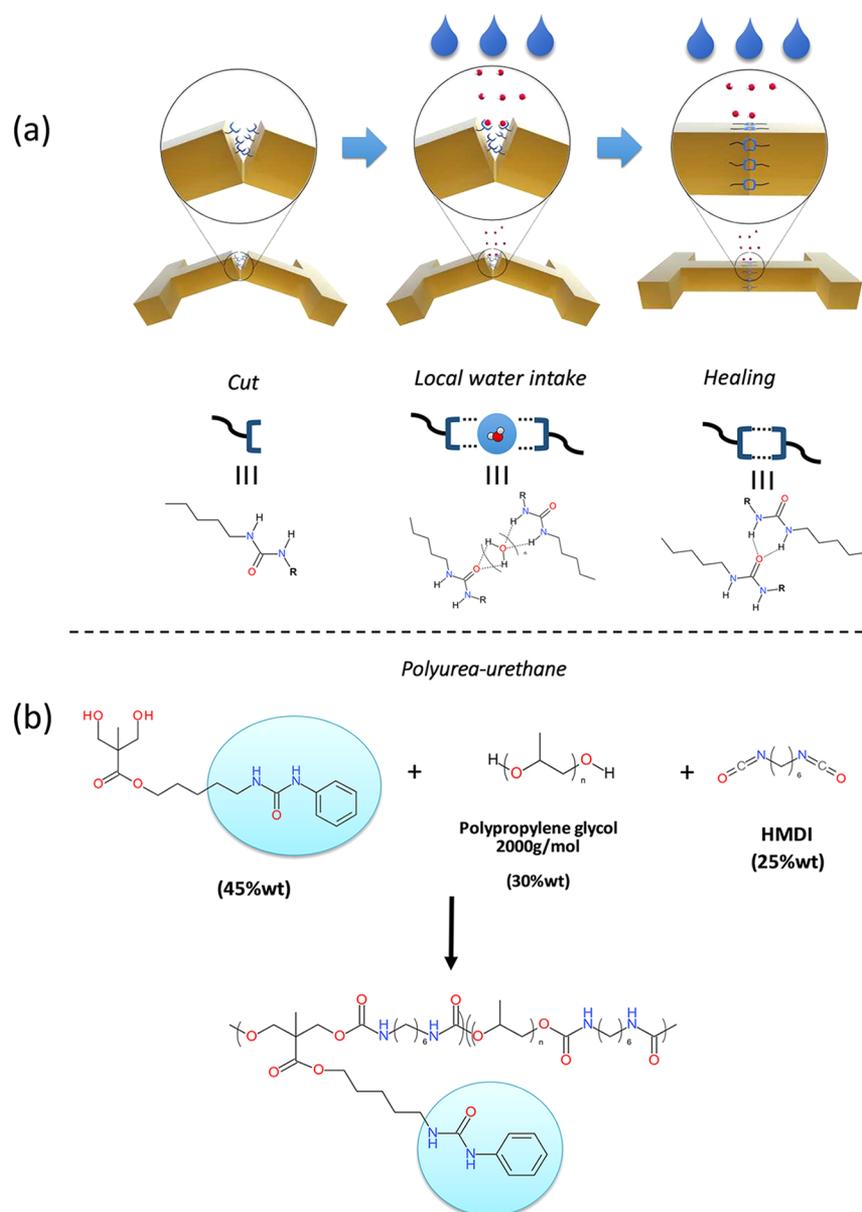
Figure 1. Schematic representation of the proposed moisture-driven healing mechanism of the urea-based polyurethane: (i) release of freestanding urea moieties at the damage sites, (ii) establishment of hydrogen-bond bridges, as assisted by water, between the freestanding urea moieties, and (iii) reformation of intermolecular clusters between urea-based moieties as water is expelled from the non-hygroscopic polyurethane (A) and the synthetic pathway of the proposed urea-based polyurethane (B).

dynamic exchanges between boronic ester bonds.[13] Our group has also reported iminoboronate-based boroxine networks healable at ambient humidity.[14] More interestingly, Yang and Urban developed glucose-based polyurethane networks that are able to self-heal under atmospheric air by fixing CO_2 and water.[15] The self-repair process, although remains a one-shot procedure, involves the physical diffusion of cleaved network segments as well as the formation of carbonate and urethane linkages.

Herein, a robust and elegant approach on the basis of dynamic exchanges between urea moieties and water molecules to trigger local and autonomous moisture-driven healing is provided (Figure 1a). The concept described in the present paper is utterly simple; that is, once damaged, the polymeric materials release freestanding urea moieties at their surface that rapidly interact with water. Due to this dynamic exchange between urea-

based moieties and water molecules, the damaged area gets locally plasticized and progressively sealed upon the reformation of intermolecular clusters between urea-based moieties, thus favoring the release of water out of the surface.

■ RESULTS AND DISCUSSION

Mechanically robust materials that would be dynamic enough to spontaneously self-heal in the simple presence of atmospheric moisture as effectively as in biological designs are obviously targeted.[16,17] As the mobility and the hydrophobicity of the polymeric segments are of prime importance to achieve an efficient self-repair mechanism, amorphous and hydrophobic poly(propylene glycol) (PPG) is selected as the main polymeric skeleton of the proposed self-healing materials. Among the emergence of dynamic covalent and noncovalent chemistries, urea moieties appeared to us as the most appropriate motifs to

be incorporated within this polymeric segment. For example, Ying et al. demonstrated the importance of urea substituents by introducing hindered functionalities that led to dynamic covalent urea bonds for self-healing polymers purposes.[18] Such materials possess a hydrogen-bonding motif via its urea bond that can increase the mechanical strength of polymers, a property that most other dynamic covalent chemistries lack. Since the determination of hydrogen-bond strength involving urea substituents is not straightforward,[19] a selection of urea candidates was subjected to DFT calculations in order to assess the stabilization energy associated with the formation of model dimers formed by two adjacent units (Figures S1a,b and Table S1). Urea–urea interaction strengths of different ureas α-substituted with hydrogen, methyl, pentyl, cyanide, or phenyl and α'-substituted with pentyl groups are thus estimated. The results show that urea α-substituted with the phenyl group yields good compromises between the high interaction strength required and the easiness from a synthetic viewpoint. As such, α-phenyl-α'-pentylurea functionalities are selected and incorporated at high concentration (i.e., 9:1 urea-based diol:PPG ratio) into the PPG-based polyurethane backbone using hexamethylene diisocyanate (HMDI) as a coupling agent (Figure 1b and Figures S2a–c and S3a,b). It results in a non-hygroscopic PPG-based polyurethane characterized by a glass transition temperature below room temperature (i.e., T_g of 12 °C). Although the as-synthesized urea-based polyurethane is fully water-insoluble (an insoluble fraction of ~100% in water, Table S2), the latter is able to trap some water molecules when exposed at ambient humidity (a water intake of ~2.8 wt %, Figure S4). As a result, when exposed at ambient humidity (i.e., 45% of relative humidity), the resulting urea-based polyurethane films healed within ~18 h (Figure 2a,b). Note that the complete healing could be further repeated (more than twice) with the same efficiency. When exposed to higher relative humidity (RH) though, the complete healing is even faster. As such, the polyurethane healed within ~7 and 4 h when exposed at RH 69 and RH 97% (Figure S5), respectively. Although only a very limited impact on T_g of the urea-based polyurethanes is observed during the healing process (Table S3), allowing us to exclude any bulk water-induced plasticization,[20,21] we expected that healing is the result of a local plasticizing effect at the damaged sites where freestanding urea moieties are abundant. To provide clear evidence on the role of water in the healing process, two controlled experiments are conducted, either on urea-based polyurethanes in a dried nitrogen atmosphere (i.e., absence of water) (Figure 2c,d) or on non-urea-based polyurethanes (i.e., only having benzyl pendant moieties) exposed at ambient humidity (Figures S6–S8), and no healing is observed. In contrast, interfacial healing could be achieved in our urea-based polyurethanes after cutting a 0.5 cm diameter rod in two pieces and putting them back 30 s in contact at 45% RH (Figure S9). Once recovered, the rod could be further lengthened up to 12 times of its initial length without any rupture in the healed section. Comparison of Young's moduli of undamaged and moisture-driven healed films (i.e., 18 h at 32% HR) qualitatively assessed the healing performance, which is found to be higher than 97% (Figure S10a,b).[22] While urethane bonds present along the backbone do not seem to participate in the healing process, we attributed the recovery of the interfacial strength to the establishment of hydrogen-bond bridges, as assisted by water, between freestanding urea moieties at the damaged sites. Since freestanding urea groups are only abundant around the damaged areas, no adhesion is observed when two
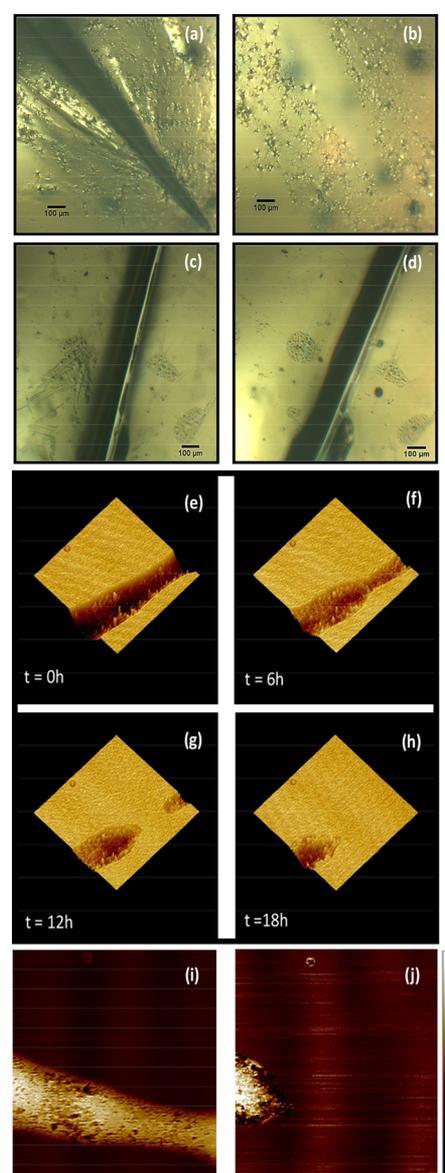

Figure 2. Scratch healing behavior of the proposed urea-based polyurethane immediately after the damage (A,C) and after being exposed to ambient humidity (B) or dried nitrogen atmosphere (D). Three-dimensional AFM topography images after different healing times (E–H) (scan size: 3.5 μm). Adhesion mapping using nanoindentation immediately after the damage (I) and after being healed (J) (scan size: 3.5 μm, scale bar ranging from 100 pN to 15 nN).

undamaged polyurethanes are brought together (Figure S11). Interestingly, Leibler and co-workers demonstrated that the number of freestanding urea bonds available for healing decreases with time due to hydrogen-bond reassociation.[23] The above mechanism obviously limits the healing efficiency if the sample is not mended immediately after being broken but only after some waiting time. A similar approach is thus used to highlight the role of water in the healing mechanism of our urea-based polyurethanes. After being cut into two distinctive pieces, the broken parts are kept apart for 24 h in either a dry (i.e., 10% RH) or an ambient (i.e., 40% RH) atmosphere and subsequently mended for 24 h at 40% RH. While the samples kept under a dry atmosphere still exhibited freestanding urea groups that can fully participate in the healing process once re-exposed to moisture (with a healing efficiency of 97%), urea moieties present at the
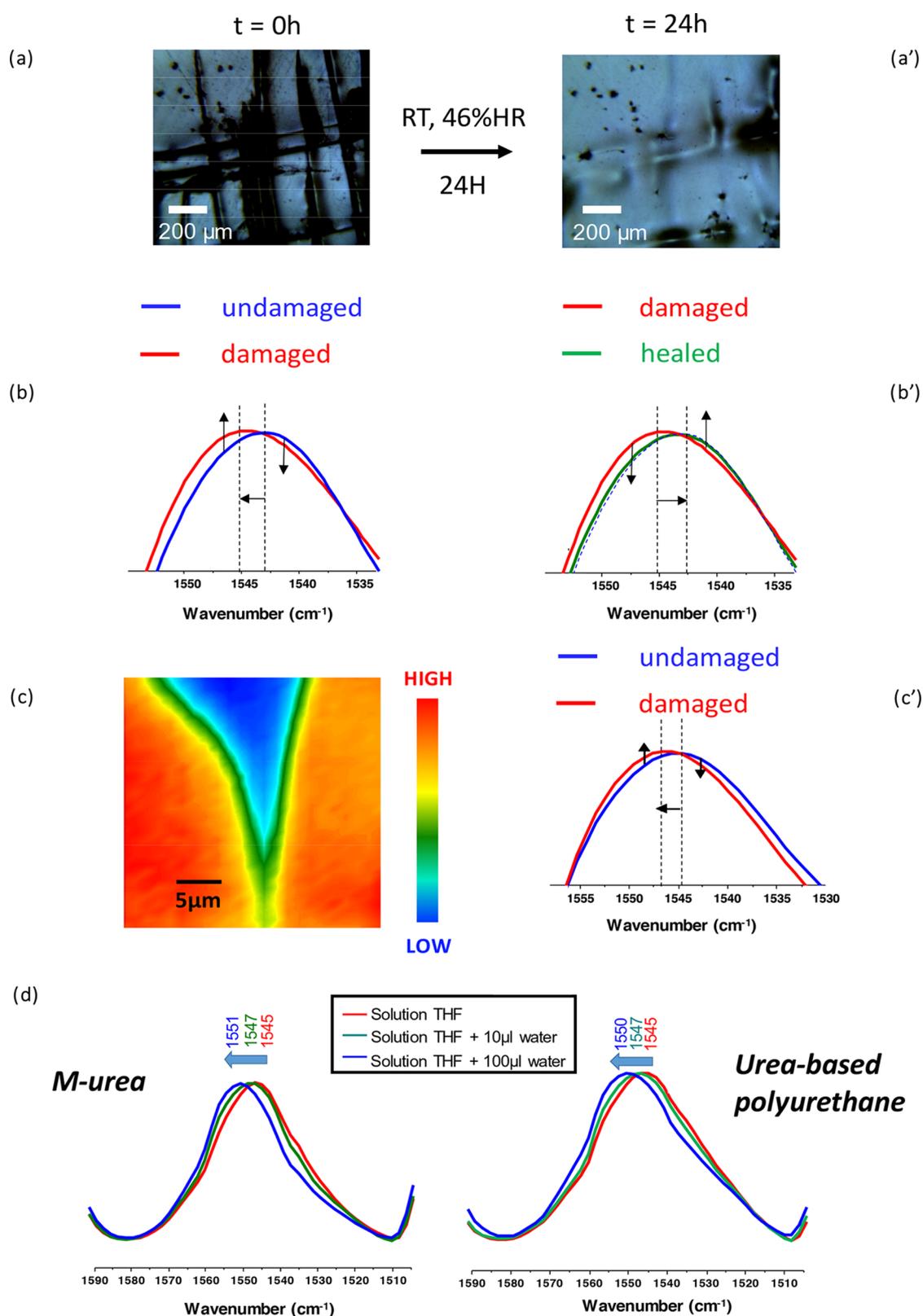
Figure 3. Theoretical and experimental investigation of the urea−water-based self-healing mechanism. Optical microscope images of severely damaged (A) and healed (A') samples as well as the IR imaging of the damaged urea-based polyurethane (C) with their respective ATR-FTIR vibrational changes centered on urea amide II region (B, B', and C', respectively). The colors represent the intensity distribution of vibrational band centered at 1545 cm^{-1} (red and blue colors represent high and low intensities of the selected band, respectively). ATR-FTIR spectra centered on the urea bending mode for M-urea (left) and the urea-based polyurethane (right) in THF solution containing an increasing amount of water (D).

freshly cut surfaces readily interact with water when placed under ambient conditions, promoting hydrogen-bond reassoci-

ation so that no free groups remain available for bridging the two broken parts together and the healing is no longer possible

(Figure S12a,b). The latter clearly supports that freestanding groups are generated on the freshly damaged surface, though water is required to assist the reassociation of freestanding urea bonds. All in all, hydrogen-bond reassociation is considered to be part of the mending mechanism.

Using peak-force tapping atomic force microscopy (PFT-AFM), various mechanical properties at the nanoscale such as adhesion or deformation are simultaneously measured and related to the topography (Figure 2e–j).[24] The healing process is thought to proceed through a "zipping effect". Time-lapse AFM is therein used for direct visualization of the nanoscale dynamics as a function of healing time (Movie S1). As such, the inner depth of the cut is reduced during the initial healing stage, forming a zipper-like pattern that cements the damage over time. The latter suggests that the damage is filled by interfacial flow (as assisted by local water-induced plasticization) followed by hydrogen-bond reassociation.[2] Herein, topographic images showed almost complete healing from ~18 h (up to 97% recovery of undamaged strength) (Figure 2e–h). Besides, adhesion images attested to the restoration of the nano-mechanical properties after healing (Figure 2i,j). Note that the presence of freestanding urea groups at the freshly cut surfaces can even induce higher adhesion at the healed areas than the undamaged ones. To gain a deeper and local insight into the chemical environment at the surface (ca. 1 μm depth), we further investigated the water–urea interactions both in the solid state and solution by means of ATR-FTIR measurements on various reference systems. Since the band interpretation in the amide II region (1500−1600 cm^{-1}) is not straightforward for our urea-based polyurethane,[25] extra DFT calculations are used. First, a model molecule having similar urea-based functionalities to our urea-based polyurethane, that is, M-urea (see the synthesis details on Figure S2), is investigated. Recall that rapid dynamic exchanges between freestanding urea moieties and moisture in the damaged areas are considered to be the healing mechanism of the urea-based polyurethane (Figure 1a). This mechanism is supported by molecular dynamics simulations on a large system made of 100 water molecules randomly located around 10 molecules of M-urea. After a 100 ps dynamic run performed at room temperature (NVT), large and small urea–water clusters tend to spontaneously form, with the water playing the role of a linker within those clusters (Figure S13). Here, water is a necessary environmental assistant of the healing chemistry. Likewise, catechol–Fe^{3+} coordinate bonds are found to be dynamic in the presence of seawater, while the dynamism is immobilized after removing water.[7] The spontaneous urea–water interaction allowing structural dynamics around two urea groups is then subsequently investigated by DFT calculations. In the presence of water molecules, the theoretical frequency of the urea bending vibration shifts toward higher wavenumbers (i.e., from 1545 to 1550 cm^{-1}), attributed to the increase of the vibration frequency in the hydrogen-bonded N−H⋯O group (Figure S14a). Note that these theoretical predictions are consistent with Leibler et al. reporting the use of infrared spectroscopy to study the dissociation of urea hydrogen bonds with temperature.[23] To discriminate hydrogen-bonded urea interacting with either water or carbonyls (related to urea or urethane), theoretical frequencies of urea bending were thus calculated on molecular models strictly mimicking the pendant α-phenyl-α'-pentylurea functionalities of the urea-based polyurethane (Figure S14b). Urea bending vibration appeared at a much higher wavenumber (i.e., 5 cm^{-1} higher) when interacting with water (i.e., 1552

cm^{-1}) than with carbonyls (i.e., 1546 cm^{-1} with urea and 1547 cm^{-1} with urethane). ATR-FTIR spectra are then collected on (i) undamaged, (ii) severely damaged, and (iii) healed urea-based polyurethanes. Herein, the urea band reversibly shifted in wavenumber when the sample is damaged (Figure 3a,b) and subsequently healed (Figure 3a',b'), which is most likely attributed to the synchronous decrease and increase of free- and H-bonded urea band intensity, respectively. While the polymeric materials release freestanding urea moieties that rapidly interact with the surrounding moisture when damaged, the undamaged ones did not exhibit such a shift since no (or less) freestanding urea moieties were available at their surface. Note that reversible hydrogen debonding/rebonding of urethane and ester groups is further observed upon damage–repair cycles, suggesting that the damage energy is most likely dissipated by hydrogen-bond cleavage (Figure S15). To complement ATR-FTIR observations, internal reflection IR imaging allowing a spatial resolution of about 1 μm^2 is conducted.[15,26,27] Focusing on the 1545 cm^{-1} region, the variation of band intensity is pointing toward a higher wavenumber at the damage site, confirming the release of freestanding urea moieties after damage (Figure 3c and Figure S16). Controlled ATR-FTIR experiments on undamaged and damaged samples in contact with water (i.e., RH 100%) further illustrated the same vibrational energy changes as those observed under ambient conditions (Figure S17a,b). A peculiar attention was paid to control experiments with M-urea and the urea-based polyurethane in solution in THF with increasing amount of water. As a result, the maximum of the urea band vibration shifted toward higher wavenumbers (i.e., from 1545 to 1551 cm^{-1} for M-urea and from 1545 to 1550 cm^{-1} for the urea-based polyurethane) as the amount of water increases in the THF solution, supporting the spontaneous formation of specific urea–water interactions (Figure 3d). Herein, the perfect agreement between theoretical and experimental data clearly demonstrated the prominent role of water in the healing process. Since the presence of a large amount of water did not affect the urethane signals at 1710 and 1680 cm^{-1} of the urea-based polyurethane, we can further conclude that water molecules exclusively interact with urea moieties due to more favored interactions than those with urethane moieties (Figure S18).[28] This exclusive interaction of water with pending urea groups of the resulting urea-based polyurethane is further confirmed by ^{1}H NMR in deuterated DMF with an increasing amount of deuterated water (from 0 to 50 μL of D$_2$O, Figure S19a,b). Although peaks related to the urea functionalities are unshielded, their intensities progressively dropped upon the addition of D$_2$O, confirming that the chemical environment of the urea groups is affected by water. The latter is not observed on urethane groups of non-urea-based polyurethane (i.e., with benzyl functionalities).

Since freestanding urea-based moieties having very high affinity with water are abundant at the damaged sites, we envisioned that the broken parts can, to a certain extent, act as a "sponge" when exposed to humidity. The latter is fully reflected by microbalance tests under different relative humidities (Figure 4). When damaged and undamaged samples exposed to RH 0% and RH 50% behave similarly (with a low water intake of ca. 2 wt % at RH 50%), the damaged sample gave a positive water intake of about +3 wt % at RH 100% compared to the undamaged one (ca. 7 wt % vs ca. 4 wt %, respectively). Recall that rapid dynamic exchanges between urea-based moieties and moisture at the damage sites promote a local and spontaneous healing response
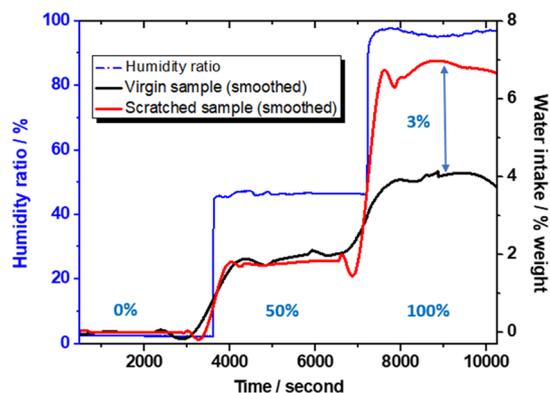
Figure 4. Water intake of the damaged and undamaged samples when exposed to different relative humidities. Samples (20 μm) are exposed for 1 h at each relative humidity (successively at RH 0%, RH 50%, and RH 100%).

to damage. Since no (or less) freestanding urea moieties are available on undamaged surfaces, only a slight water intake occurred due to water diffusion through the material. Besides, exposing damaged materials to RH 100% and subsequently to RH 50% led to the release of the positive water intake (ca. 3 wt %), promoting the reassociation of freestanding urea bonds for bridging the two broken parts together.

CONCLUSIONS

Urea-based polyurethanes with spontaneous moisture-driven healing properties in the presence of environmental water are demonstrated. Herein, a complete and efficient moisture-driven healing in the proposed urea-based polyurethane is constructed around rapid dynamic exchanges between freestanding urea moieties and water in response to damage. The healing mechanism is related to the formation of water−urea clusters as supported by molecular dynamics simulations and by DFT/FTIR coupled studies. Obviously, the present concept paves the way to the design of a plethora of new spontaneous water-responsive materials.

EXPERIMENTAL SECTION

The synthetic details for the monomers and polymers are reported in Figures S2 and S3. All chemicals were purchased from Sigma Aldrich and VWR. Calculations of the urea vibrational frequencies were performed at the DFT level using the B3LYP[29−31] functional and a 6-31G(d,p) basis set on DFT-optimized structures at the same level of theory (except that the D3 version of Grimme's dispersion with Becke−Johnson damping[32] was used in the first case to properly account for the intermolecular interactions between water and urea functionalities). All DFT calculations were performed within the Gaussian09 package (Figures S1 and S9).[33] All molecular dynamics simulations were performed using the Materials Studio 7.0 software (Section S14).[34] Tensile tests were performed using a Zwick universal tensile testing machine (speed = 5 mm min^{-1} and preload = 0.03 N) (Figures S12 and S13). Thermogravimetric analyses (TGA) were performed using a TGA Q500 TA Instruments under nitrogen with a heating rate of 20 °C min^{-1} from room temperature to 800 °C. Differential scanning calorimetry (DSC) measurements were carried out using a DSC Q2000 TA Instruments with a modulated heat/cool/heat program from −80 to 100 °C at 10 °C min^{-1}. FTIR spectra were recorded on an ATR-mode Bruker Tensor 27 spectrometer from 4000 to 600 cm^{-1} (spectral resolution of 1 cm^{-1}). Experiments reported in Figure 3 were recorded using a micro-attenuated total reflectance Fourier transform infrared spectra (μATR FTIR) (Agilent Cary 680 FTIR single-beam spectrometer setting at 4 cm^{-1} resolution). A diamond crystal, with a

constant contact pressure between the crystal and the specimens, was used. Each experiment was repeated several times to confirm that the changes are consistent and are due to the damage−repair cycle (Figure S16). All spectra were normalized using the band at 1000 cm^{-1} corresponding to the ether stretching frequency, which is not affected by the healing process. Internal reflection IR images (IRIRI) were obtained using a Cary 600 series Stingray system equipped with internal reflection IR imaging providing a 1 mm spatial resolution (Figure S17). This system consists of a Cary 680 spectrometer, a Cary 620 FTIR microscope, an image IR focal plane array (FPA) image detector, and a germanium (Ge) imaging crystal. Traces showing IR spectra inside and outside the damaged area were averaged over 20 spectra. Self-healing experiments were performed on 300 μm thick films using a Leica DMRXP optical microscope. Films were cut over their entire thickness, using an FA fresh razor blade and exposed to different degrees of relative humidity: RH 97% (saturated solution of KNO_3), RH 69% (saturated solution of NaCl), and RH 45% (ambient humidity). Contact angles were measured with a DSA 10-Mk2 tensiometer (Krüss), and the analysis was replicated five times with a drop of 20 μL of water. Quartz microbalance tests were performed using a homemade microbalance tester described in detail in Figure S20. Atomic force microscopy (AFM) experiments were carried out using Bruker Dimension Icon (Santa Barbara, CA) equipment in peak-force tapping mode at a relative humidity of 25%. The silicon nitride lever (SNL) cantilever has a spring constant of 0.12 N m^{-1}. The frequency rate for the force curve acquisition was 2 kHz, and the number of pixels was 512 × 512. NanoScope Analysis 1.80 software was used for the data analysis.

ASSOCIATED CONTENT

Ⓢ Supporting Information

The Supporting Information is available free of charge at https://pubs.acs.org/doi/10.1021/acsami.9b16858.

> Synthesis of urea-based polyurethanes and polyurethanes bearing benzyl pendant group as reference, swelling tests, water intake on damaged and undamaged polyurethanes, moisture-dependent healing tests, mechanical testing on healed polyurethanes, ATR-FTIR experiments, IR imaging, molecular dynamics simulations, theoretical vibration frequency, and estimation of the urea−urea interaction strength by DFT calculations (PDF)

> Movie on time-lapse AFM for direct visualization of the nanoscale dynamics (AVI)

AUTHOR INFORMATION

Corresponding Author
*E-mail: jean-marie.raquez@umons.ac.be.

ORCID Ⓘ
Jeremy Odent: 0000-0002-3038-846X
Jérôme Cornil: 0000-0002-5479-4227
Jean-Marie Raquez: 0000-0003-1940-7129

Notes
The authors declare no competing financial interest.

ACKNOWLEDGMENTS

■ REFERENCES

(1) Cremaldi, J. C.; Bhushan, B. Bioinspired Self-Healing Materials: Lessons from Nature. *Beilstein J. Nanotechnol.* **2018**, *9*, 907−935.

(2) Yang, Y.; Ding, X.; Urban, M. W. Chemical and Physical Aspects of Self-Healing Materials. *Prog. Polym. Sci.* **2015**, *49-50*, 34−59.

(3) Yang, Y.; Urban, M. W. Self-Healing Polymeric Materials. *Chem. Soc. Rev.* **2013**, *42*, 7446−7467.

(4) Wittmer, A.; Brinkmann, A.; Stenzel, V.; Hartwig, A.; Koschek, K. Moisture-Mediated Intrinsic Self-Healing of Modified Polyurethane Urea Polymers. *J. Polym. Sci., Part A: Polym. Chem.* **2018**, *56*, 537−548.

(5) Wittmer, A.; Wellen, R.; Saalwächter, K.; Koschek, K. Moisture-Mediated Self-Healing Kinetics and Molecular Dynamics in Modified Polyurethane Urea Polymers. *Polymer* **2018**, *151*, 125−135.

(6) Wilker, J. J. Self-Healing Polymers: Sticky When Wet. *Nat. Mater.* **2014**, *13*, 849−850.

(7) Xia, N. N.; Xiong, X. M.; Wang, J.; Rong, M. Z.; Zhang, M. Q. A Seawater Triggered Dynamic Coordinate Bond and Its Application for Underwater Self-Healing and Reclaiming of Lipophilic Polymer. *Chem. Sci.* **2016**, *7*, 2736−2742.

(8) Ahn, B. K.; Lee, D. W.; Israelachvili, J. N.; Waite, J. H. Surface-Initiated Self-Healing of Polymers in Aqueous Media. *Nat. Mater.* **2014**, *13*, 867−872.

(9) Yesilyurt, V.; Webber, M. J.; Appel, E. A.; Godwin, C.; Langer, R.; Anderson, D. G. Injectable Self-Healing Glucose-Responsive Hydrogels with Ph-Regulated Mechanical Properties. *Adv. Mater.* **2016**, *28*, 86−91.

(10) Jeon, I.; Cui, J.; Illeperuma, W. R. K.; Aizenberg, J.; Vlassak, J. J. Extremely Stretchable and Fast Self-Healing Hydrogels. *Adv. Mater.* **2016**, *28*, 4678−4683.

(11) Li, L.; Yan, B.; Yang, J.; Chen, L.; Zeng, H. Novel Mussel-Inspired Injectable Self-Healing Hydrogel with Anti-Biofouling Property. *Adv. Mater.* **2015**, *27*, 1294−1299.

(12) Liu, M.; Liu, P.; Lu, G.; Xu, Z.; Yao, X. Multiphase-Assembly of Siloxane Oligomers with Improved Mechanical Strength and Water-Enhanced Healing. *Angew. Chem.* **2018**, *130*, 11242−11416.

(13) Cash, J. J.; Kubo, T.; Bapat, A. P.; Sumerlin, B. S. Room-Temperature Self-Healing Polymers Based on Dynamic-Covalent Boronic Esters. *Macromolecules* **2015**, *48*, 2098−2106.

(14) Delpierre, S.; Willocq, B.; De Winter, J.; Dubois, P.; Gerbaux, P.; Raquez, J.-M. Dynamic Iminoboronate-Based Boroxine Chemistry for the Design of Ambient Humidity-Sensitive Self-Healing Polymers. *Chem. − Eur. J.* **2017**, *23*, 6730−6735.

(15) Yang, Y.; Urban, M. W. Self-Repairable Polyurethane Networks by Atmospheric Carbon Dioxide and Water. *Angew. Chem., Int. Ed.* **2014**, *53*, 12142−12147.

(16) Roy, N.; Bruchmann, B.; Lehn, J.-M. Dynamers: Dynamic Polymers as Self-Healing Materials. *Chem. Soc. Rev.* **2015**, *44*, 3786−3807.

(17) Yanagisawa, Y.; Nan, Y.; Okuro, K.; Aida, T. Mechanically Robust, Readily Repairable Polymers Via Tailored Noncovalent Cross-Linking. *Science* **2018**, *359*, 72−76.

(18) Ying, H.; Zhang, Y.; Cheng, J. Dynamic Urea Bond for the Design of Reversible and Self-Healing Polymers. *Nat. Commun.* **2014**, *5*, 3218.

(19) Gilli, P.; Pretto, L.; Bertolasi, V.; Gilli, G. Predicting Hydrogen-Bond Strengths from Acid−Base Molecular Properties. The Pka Slide Rule: Toward the Solution of a Long-Lasting Problem. *Acc. Chem. Res.* **2009**, *42*, 33−44.

(20) Pissis, P.; Apekis, L.; Christodoulides, C.; Niaounakis, M.; Kyritsis, A.; Nedbal, J. Water Effects in Polyurethane Block Copolymers. *J. Polym. Sci., Part B: Polym. Phys.* **1996**, *34*, 1529−1539.

(21) Yu, Y.-J.; Hearon, K.; Wilson, T. S.; Maitland, D. J. The Effect of Moisture Absorption on the Physical Properties of Polyurethane Shape Memory Polymer Foams. *Smart Mater. Struct.* **2011**, *20*, No. 085010.

(22) Diesendruck, C. E.; Sottos, N. R.; Moore, J. S.; White, S. R. Biomimetic Self-Healing. *Angew. Chem., Int. Ed.* **2015**, *54*, 10428−10447.

(23) Cordier, P.; Tournilhac, F.; Soulié-Ziakovic, C.; Leibler, L. Self-Healing and Thermoreversible Rubber from Supramolecular Assembly. *Nature* **2008**, *451*, 977−980.

(24) Khelifa, F.; Habibi, Y.; Leclére, P.; Dubois, P. Convection-Assisted Assembly of Cellulose Nanowhiskers Embedded in an Acrylic Copolymer. *Nanoscale* **2013**, *5*, 1082−1090.

(25) Socrates, G. *Infrared and Raman Characteristic Group Frequencies: Tables and Charts*; John Wiley & Sons: 3rd Edition. **2004**, 366.

(26) Ghosh, B.; Urban, M. W. Self-Repairing Oxetane-Substituted Chitosan Polyurethane Networks. *Science* **2009**, *323*, 1458−1460.

(27) Otts, D. B.; Zhang, P.; Urban, M. W. High Fidelity Surface Chemical Imaging at 1000 Nm Levels: Internal Reflection Ir Imaging (Iriri) Approach. *Langmuir* **2002**, *18*, 6473−6477.

(28) Yilgör, E.; Burgaz, E.; Yurtsever, E.; Yilgör, İ. Comparison of Hydrogen Bonding in Polydimethylsiloxane and Polyether Based Urethane and Urea Copolymers. *Polymer* **2000**, *41*, 849−857.

(29) Becke, A. D. Density-Functional Exchange-Energy Approximation with Correct Asymptotic Behavior. *Phys. Rev. A* **1988**, *38*, 3098−3100.

(30) Lee, C.; Yang, W.; Parr, R. G. Development of the Colle-Salvetti Correlation-Energy Formula into a Functional of the Electron Density. *Phys. Rev. B* **1988**, *37*, 785−789.

(31) Miehlich, B.; Savin, A.; Stoll, H.; Preuss, H. Results Obtained with the Correlation Energy Density Functionals of Becke and Lee, Yang and Parr. *Chem. Phys. Lett.* **1989**, *157*, 200−206.

(32) Grimme, S.; Ehrlich, S.; Goerigk, L. Effect of the Damping Function in Dispersion Corrected Density Functional Theory. *J. Comput. Chem.* **2011**, *32*, 1456−1465.

(33) Frisch, M. J.; Trucks, G. W.; Schlegel, H. B.; Scuseria, G. E.; Robb, M. A.; Cheeseman, J. R.; Scalmani, G.; Barone, V.; Mennucci, B.; Petersson, G. A.; Nakatsuji, H.; Caricato, M.; Li, X.; Hratchian, H. P.; Izmaylov, A. F.; Bloino, J.; Zheng, G.; Sonnenberg, J. L.; Hada, M.; Ehara, M.; Toyota, K.; Fukuda, R.; Hasegawa, J.; Ishida, M.; Nakajima, T.; Honda, Y.; Kitao, O.; Nakai, H.; Vreven, T.; Montgomery, Jr., J. A.; Peralta, J. E.; Ogliaro, F.; Bearpark, M. J.; Heyd, J.; Brothers, E. N.; Kudin, K. N.; Staroverov, V. N.; Kobayashi, R.; Normand, J.; Raghavachari, K.; Rendell, A. P.; Burant, J. C.; Iyengar, S. S.; Tomasi, J.; Cossi, M.; Rega, N.; Millam, N. J.; Klene, M.; Knox, J. E.; Cross, J. B.; Bakken, V.; Adamo, C.; Jaramillo, J.; Gomperts, R.; Stratmann, R. E.; Yazyev, O.; Austin, A. J.; Cammi, R.; Pomelli, C.; Ochterski, J. W.; Martin, R. L.; Morokuma, K.; Zakrzewski, V. G.; Voth, G. A.; Salvador, P.; Dannenberg, J. J.; Dapprich, S.; Daniels, A. D.; Farkas, Ö.; Foresman, J. B.; Ortiz, J. V.; Cioslowski, J.; Fox, D. J. *Gaussian 09*; Gaussian, Inc.: Wallingford, CT, USA, 2009.

(34) *Ms Modeling Ver. 7.0.200.0*; Accelrys: San Diego, CA, USA, 2013.